Radiation Physics and Chemistry 218 (2024) 111564

Contents lists available at ScienceDirect

Radiation Physics and Chemistry

journal homepage: www.elsevier.com/locate/radphyschem

A dosimetric study of occupational exposure during computed tomography procedures

Monique F. Silva [a], Ana L.O. Caixeta [a], Samara P. Souza [a], Otávio J. Tavares [a], Paulo R. Costa [b], William S. Santos [a,c], Lucio P. Neves [a,c], Ana P. Perini [a,c,*]

[a] Postgraduate Program in Biomedical Engineering (PPGEB), Faculty of Electrical Engineering, Federal University of Uberlândia, MG, Brazil
[b] Institute of Physics, University of Sao Paulo, São Paulo, SP, Brazil
[c] Institute of Physics, Federal University of Uberlândia, Uberlândia, MG, Brazil

ARTICLE INFO

Handling Editor: Dr. Chris Chantler

Keywords:
CT exams
Chest
Personal dosimetry
Monte Carlo simulation

ABSTRACT

The number of chest computed tomography (CT) procedures has increased worldwide as it is a diagnostic tool for a variety of lung diseases, mainly for visualizing and monitoring lung extensions and impairments. Due to respiratory problems in patients during the CT scan, health professionals need to perform special care such as Bag-Valve-Mask Ventilation and accompany them throughout the procedure. Therefore, this study aimed to investigate and evaluate the doses received by these professionals during a chest CT study. The effectiveness of personal protective equipment (PPE) was also evaluated. To achieve these objectives, computational scenarios were simulated with pediatric (1 and 10 years old) and adult virtual anthropomorphic phantoms, representing patients and professionals. Conversion coefficients for equivalent (CC[H_T]) and effective (CC([E]) doses were determined using the MCNP 6.2 Monte Carlo code. The results obtained showed that the highest dose effective [E] values were for the professional positioned in front of the gantry and without the use of PPE, ranging from around 5.78×10^{-2} to 1.82×10^{-1} mSv, depending on the patient size monitored during the examination and the x-ray tube voltage. The organs of the simulated professionals with the highest CC[H_T] values were the breasts (female) and testicles (male). Furthermore, the use of PPE demonstrate reductions on CC[H_T] and CC([E] values of the professional of approximately 91 %.

1. Introduction

Some patients with respiratory system problems require special care and respiratory equipment, such as the manual ventilation mechanism bag valve mask (BVM) during the performance of a computed tomography (CT) exam. In such cases, the presence of a trained professional to provide necessary care is essential (Nagamoto et al., 2021). There are also other procedures that lead the professional to accompany or contain patients, such as in pediatric procedures, and special care in patients with multiple traumas (Nagamoto et al., 2021; Mori et al., 2014; Al-Hal et al., 2003; Kobayashi et al., 2012; Sookpeng et al., 2019). Mori et al. (2014) pointed out that, on average, one to two times per month, the professionals needed to accompany and remain in the CT room during the exam, and that 30 % of the professionals felt anxious when performing manual ventilation (Mori et al., 2014).

The process of obtaining images of the lungs requires the control of the air entering and leaving the lungs, which the professional performing the ventilation on the patient does manually. Therefore, the professional stays in the room during the entire examination and is exposed to ionizing radiation scattered from the patient. Studies have pointed out that, in cases of professionals exposed to radiation during their workday, dermatitis, skin cancer, leukemia, cataracts, and brain tumors (Linet et al., 2010; Tamam et al., 2023; Vaño et al., 1998; Abuelhia and Alghamdi, 2020; Ferrari et al., 2010, 2019, 2022). However, there are few studies about the doses of ionizing radiation received by professionals who remain in the room during conventional CT examinations (Nagamoto et al., 2021; Heilmaier et al., 2016; Palm and Frida, 2017).

Experimental studies have investigated doses in the eye lenses of professionals performing special care, such as manual breathing on patients during diagnostic CT examinations, using radio-photoluminescent glass dosimeters (RPLD) (Nagamoto et al., 2021; Ota et al., 2021; Osanai et al., 2021). These studies highlighted a 50–92 % efficiency of lead eyewear (composed of lead glass) and the importance of their use by the

* Corresponding author. Institute of Physics, Federal University of Uberlândia, Uberlândia, MG, Brazil.
E-mail address: anapaula.perini@ufu.br (A.P. Perini).

https://doi.org/10.1016/j.radphyschem.2024.111564
Received 13 October 2023; Received in revised form 26 December 2023; Accepted 29 January 2024
Available online 1 February 2024

Table 1
Main characteristics of pediatric (1 and 10 years old) and adult (FASH3 and MASH3) virtual anthropomorphic phantoms (Kramer et al., 2009; Cassola et al., 2009, 2013; De Melo Lima et al., 2011).

Characteristics	1 year old both gonads	10 years old		Adult	
		Female	Male	Female	Male
Body mass (kg)	10.25	30.95	30.54	60.0	73.0
Height (m)	0.76	1.38	1.38	1.63	1.76
Body-Mass Index (kg/m^2)	17.73	16.23	16.01	22.7	23.6

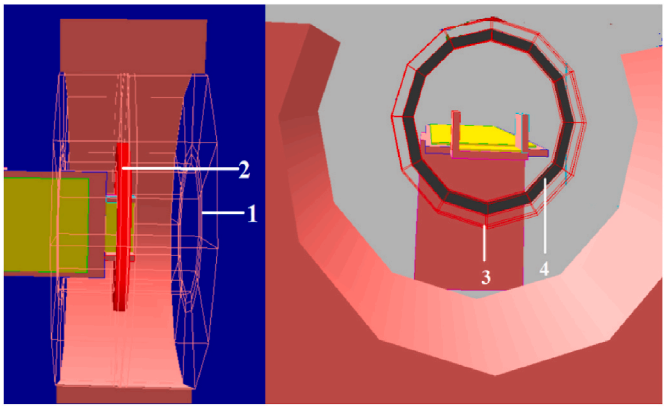

Fig. 1. CT source geometry: (1) gantry cover; (2 and 3) collimators; (4) circular X-ray source.

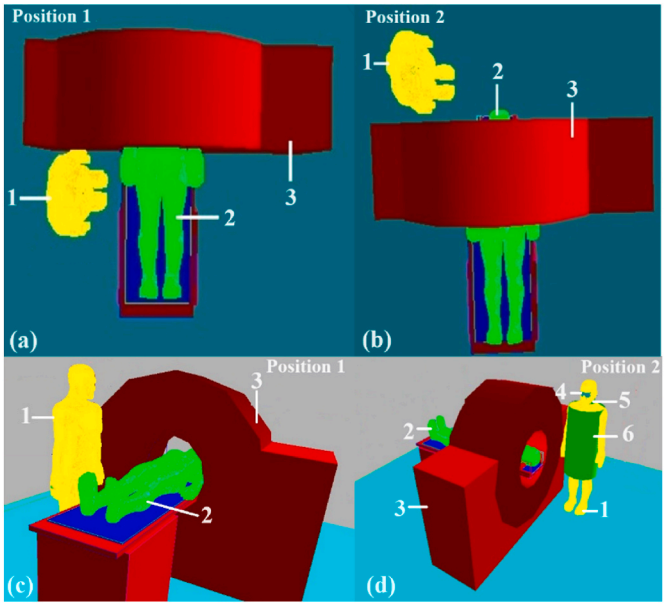

Fig. 2. Occupational exposure scenario, in which the professional (1) was positioned in front of the gantry and facing the patient table (position 1), and behind the laterally directed gantry (position 2) accompanying the patient (2) during the exam with a CT scan (3). The professional is wearing the PPE: (4) lead eyewear; (5) thyroid shield; (6) lead apron.

medical team during the CT examination. Another study by Palm and Nelson (2017) found that the position that presented the highest doses of scattered radiation was in front of the gantry, with values of 96.03 μGy during a chest examination (Palm and Frida, 2017).

Although these studies are important (Nagamoto et al., 2021; Heilmaier et al., 2016; Palm and Frida, 2017; Ota et al., 2021; Osanai et al., 2021), they present limitations, mainly in the estimation of absorbed doses to organs and tissues. Currently, computational tools such as Monte Carlo techniques allow the determination of the probability of interactions of radiation with different types of materials (Yoriyaz, 2009). Additionally, virtual anthropomorphic phantoms representing the composition of tissues and organs and anatomy of the human body are available (Kramer et al., 1982, 2009; Cristy, 1980; Lee et al., 2010). Thus, it is possible to estimate the absorbed doses for each tissue and organ, and calculate the respective effective doses for professionals and patients. In the literature, studies have used Monte Carlo and virtual anthropomorphic phantoms in CT fluoroscopy (Figueira et al., 2013; Gyekye et al., 2016).

Table 2
Scanning parameters in chest CT examination (American College of Radiology).

Patient	Tube voltage (kV)	Current-time product (mAs)	Pitch	Slice thickness (cm)	N° of slices
1 yrs	100/120	100	1	0.5	32
10 yrs	100/120	100	2	0.5	24
Adults	100/120	100	2	0.5	32

However, to the best of our knowledge, there are no published studies using these computational tools to evaluate the radiation exposure of professionals accompanying the patient during conventional CT examinations. This study aimed to investigate and evaluate the doses received by professionals during chest CT scans, when they were required to be in the CT room during the examination. Our study adopted Monte Carlo simulations with adult male and female virtual anthropomorphic phantoms to represent professionals (Kramer et al., 2009; Cassola et al., 2009). The patients were represented by phantoms of different ages (1 and 10 years and adults) (Kramer et al., 2009; Cassola et al., 2009, 2013; De Melo Lima et al., 2011). This study can be used as a guide to evaluate the equivalent and effective doses received by professionals.

2. Materials and methods

2.1. Monte Carlo Method and virtual anthropomorphic phantoms

Input files (IFs) were created to simulate typical scenarios of chest CT examinations in pediatric patients (1 and 10 years old) and adults. In these scenarios, it was considered that these patients are accompanied into the CT room by a professional providing special care during the examination. The IFs were prepared to be used with the MCNP6.2 Monte Carlo code (Werner et al., 2018), and, otherwise stated, the default configuration was used. The professionals and the patients were represented by the set of virtual anthropomorphic phantoms, developed at the *Department of Nuclear Energy of the Federal University of Pernambuco* (Kramer et al., 2009; Cassola et al., 2009, 2013; De Melo Lima et al., 2011).

They were used to represent pediatric patients aged 1- and 10-years-old, as well as adult patients and professionals, which were the MASH3 (male) and FASH3 (female) phantoms (Kramer et al., 2009; Cassola et al., 2009, 2013; De Melo Lima et al., 2011). The 1-year-old virtual phantom had both male and female gonads. The adult virtual phantoms were constructed using voxels of size 0.24 × 0.24 × 0.24 cm^3, and the pediatric ones with 0.14 × 0.14 × 0.14 cm^3. The patients' characteristics are listed in Table 1.

2.2. X-ray source for the computed tomography equipment

To simulate a CT scanner, specific and detailed information is needed regarding the X-ray source, photon energy spectrum, its dimensions, materials, the entire inherent filtering system, collimators, and bowtie filter. Some of this information can be found in the CT scanner user manuals. However, the dimensions, design, and material of the bowtie

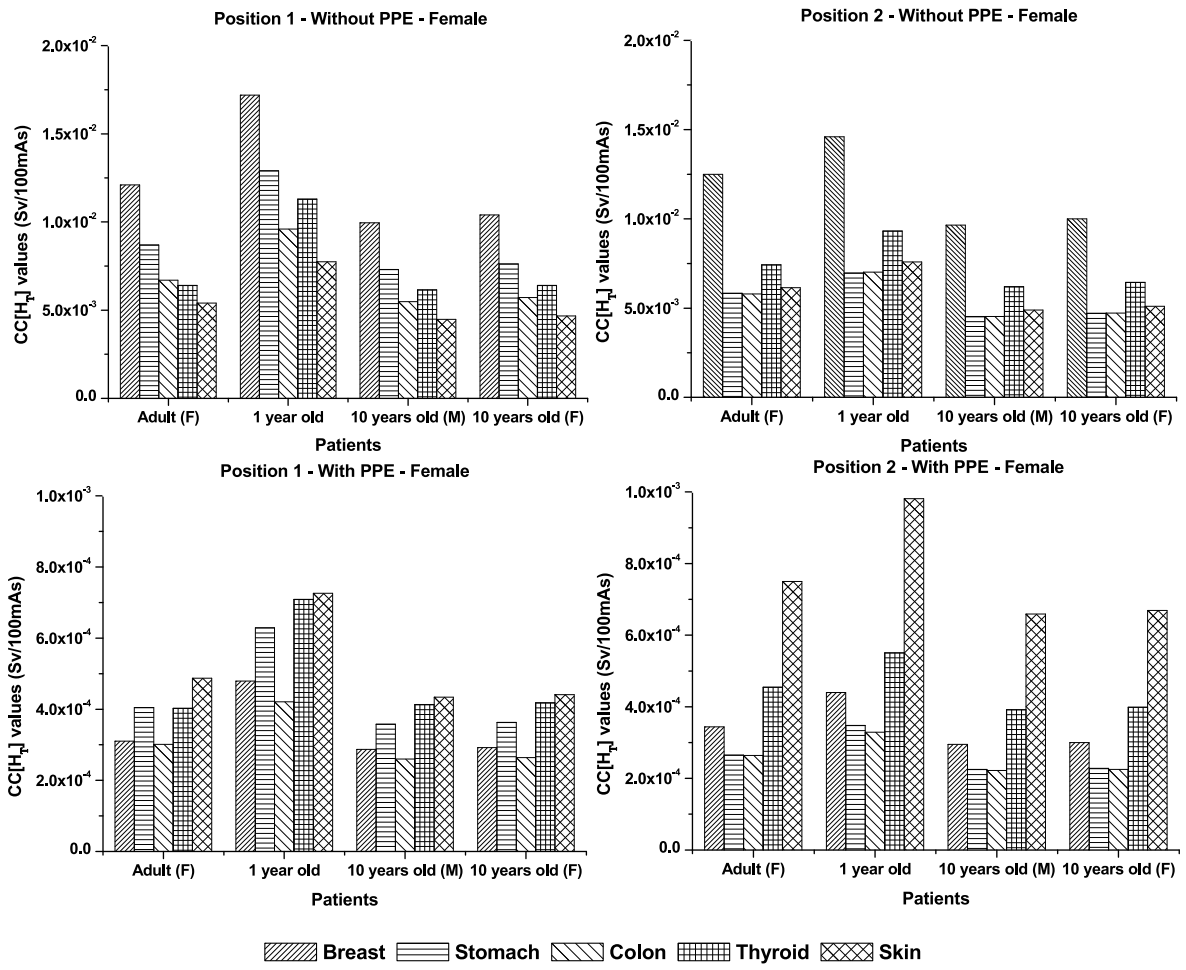

Fig. 3. Chart of the organs of the **female** professional who received the highest *CC* [H_T] values, **without** and **with** PPE in positions 1 and 2 to follow the pediatric and adult patients, during the chest CT, considering a tube voltage of 100 **kVp**.

filter are confidential and proprietary. Each scanner model has its own specifications, which makes the Monte Carlo simulation process more difficult. To overcome this problem over the years, some researchers have begun to create theoretical and experimental methods to determine the dimensions, bowtie filter models, and energy spectrum, called equivalent models (Turner et al., 2009; Boone, 2010; McKenney et al., 2011; McMillan et al., 2013).

In this study, the technical characteristics of the GE Discovery CT750HD scanner were considered, which adopted a GE Performix tungsten target X-ray tube with an anode angle of 7°, inherent filter of 6 mm aluminum (General Electric Company) and X-ray tube voltages of 100 and 120 kVp. In these cases, the bowtie filter obtained and validated by Costa et al. (2022), was used. In this study, the authors used the analytical methods of Boone (2010), to obtain the X-ray spectra and filtrations generated by the semi-empirical TBC model (Boone, 2010; Gonzales et al., 2015). The validation was performed through spectrometry and half-value layer measurements using a Compton Spectrometer, and the obtained values were compared with those in the literature (Costa et al., 2007; Terini et al., 2020).

The examination room and CT equipment were carefully simulated to mimic the real components. The material composition was established according to each chemical element and the corresponding density present in the *Compendium of Material Composition Data for Radiation Transport Modeling* (McConn et al., 2011). The walls, ceiling, and floor of the room were simulated for concrete barite-type BA ($\rho = 3.35$ g/cm^3). The internal structure of the CT Scanner is composed of steel carbon ($\rho = 7.82$ g/cm^3) and external structure made of bakelite ($\rho = 1.25$ g/cm^3).

To reproduce 360° X-ray tube rotation, the X-ray source was simulated as a volume source of ring-shaped circular geometry with a radius of 40 cm radius and 0.5 cm thickness. The entire lead collimator system ($\rho = 11.35$ g/cm^3) was also inserted into the simulation design, and the equipment was suitable for performing the examination according to the established protocols (Fig. 1).

2.3. Simulated scenarios

Typical chest CT scenarios were simulated for pediatric (1- and 10-years-old) and adult patients. All patients were accompanied by a professional to perform special care, such as manual ventilation, during the entire scan. Two of the most common positions in which the professionals stood during the procedure were selected: being in front of the gantry and facing the patient table, named position 1 (Fig. 2a), and behind the gantry directed laterally, named position 2 (Fig. 2b). The distance from the professional to the patient table was 10 cm and the distance from the gantry was 5 cm. We also considered situations with and without the use of personal protective equipment (PPE) (Fig. 2). The PPE simulated in this study was lead eyewear, lead apron, and thyroid protector, all with a thickness of 0.5 mmPb (Fig. 2c).

There are several different scanning protocols for chest CT, and many pediatric and adult patients undergo repetitive CT examinations (Ng et al., 2020; Zamani et al., 2021; Homayounieh et al., 2021). Thus, for each patient, the scan parameters were simulated according to protocols recommended and established by the *American College of Radiology* (American College of Radiology) (Table 2).

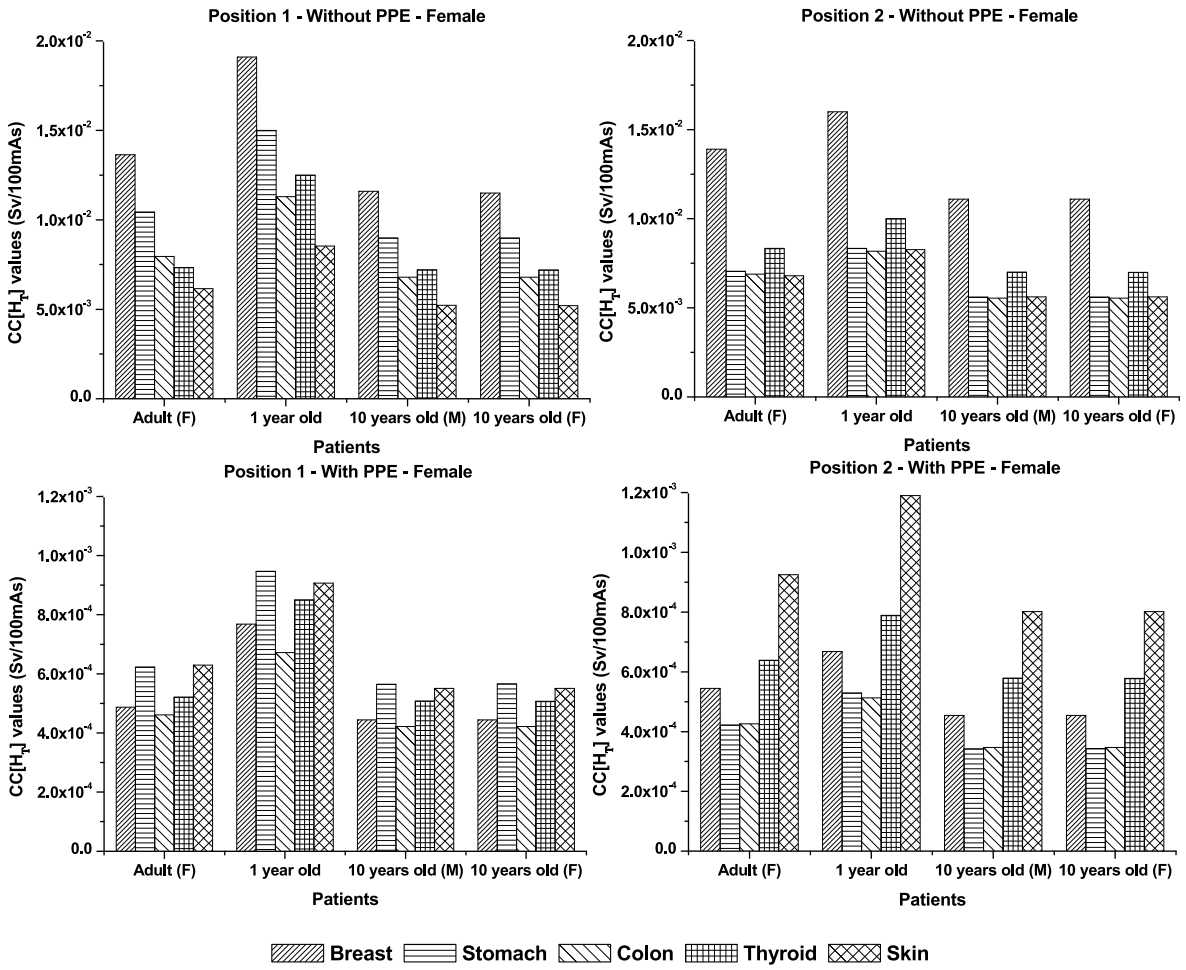

Fig. 4. Chart of the organs of the **female** professional who received the highest *CC* [H_T] values, **without** and **with** PPE in positions 1 and 2 to follow the pediatric and adult patients, during the chest CT, considering a tube voltage of **120 kVp**.

2.4. Dosimetric calculations

In the dosimetric calculations using the Monte Carlo Method, each simulation was performed with 10^9 histories, employing the *F6* tally (MeV/g/source-particle). For each CT slice, an *F6* tally was obtained, and the sum of the tally was used to calculate the conversion coefficients for equivalent (CC[H_T]) and effective (CC[E]) doses (Soares et al., 2019; ICRP, 2007). These values were obtained based on the radiation weighting factor, scan parameters, and anatomical properties of each phantom.

The CC[H_T] of the five organs that received the highest radiation doses (Figs. 3–6) was determined using equation (1), in accordance with ICRP 103, 2007 (ICRP, 2007).

$$CC[H_T] = \frac{D_T . w_R}{C_{a,100}} \quad (1)$$

where D_T is the absorbed dose obtained in MCNP 6.2, w_R is the radiation weighting factor and $C_{a,100}$ air kerma and 100 mAs. The $C_{a,100}$ was obtained computationally by simulating a pencil-type ionization chamber (Radcal Corporation, Monrovia, California 91016, USA) model 10X5-3CT, positioned at the isocenter of the gantry (Radical Corporation, 2011).

For whole-body radiation dose analysis, the *CC*[*E*] was calculated (Table 3) according to ICRP 103, 2007 (equation (2)), where w_T is the tissue weighting factor (ICRP, 2007).

$$CC[E] = \sum_T w_T \frac{CC[H_T]^{male} + CC[H_T]^{female}}{2} \quad (2)$$

To determine the effective doses (E) of professionals, it was necessary to relate the simulated scenarios to the experimentally obtained results. For this, we adopted the air kerma obtained in the study by Costa et al. (2022), which used the same CT scanner simulated in our study.

3. Results and discussion

Figs. 3–6 present the CC[H_T] values obtained by female and male professionals during the monitoring of pediatric patients (1–10 years old) and adult patients during the chest CT examination, according to the two positions of the professional, with or without PPE, and the tube voltages used (100 and 120 kVp).

Analyzing the most critical situation, in which the professional does not use any PPE, when accompanying the patients during the chest CT (Figs. 3–6), the five organs that received the highest CC[H_T] values were the breasts, stomach, thyroid, colon, and skin for the female professional, and testicles, breasts, stomach, colon, and liver for the male. This was observed for both the positions and the tube voltages evaluated in this study.

3.1. Occupational assessment

Figs. 3 and 4 show the CC[H_T] values for the female professional with and without PPE and at tube voltages of 100 kVp and 120 kVp,

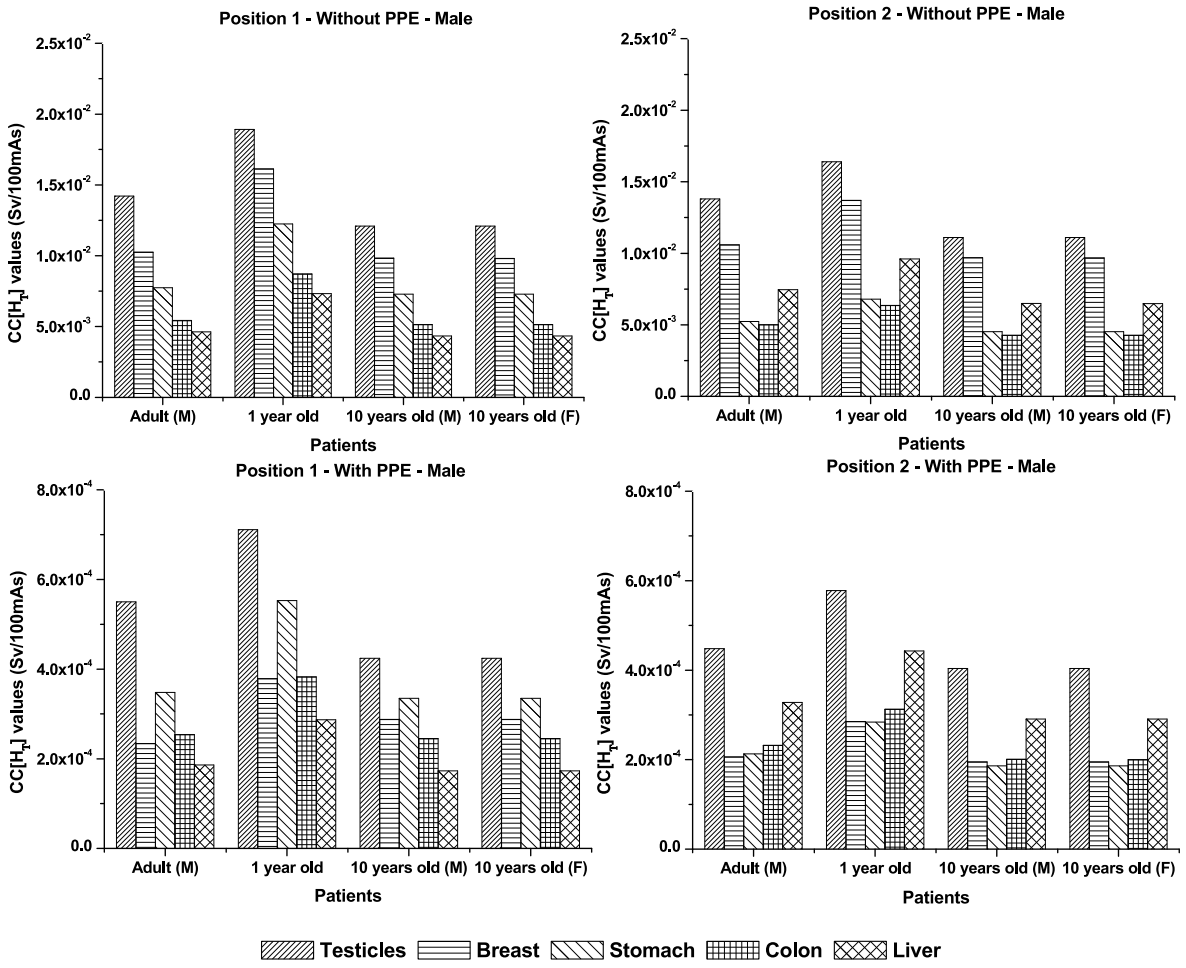

Fig. 5. Chart of the organs of the **male** professional who received the highest $CC[H_T]$ values, **without** e **with** PPE in positions 1 and 2 to follow the pediatric and adult patients, during the chest CT, considering a tube voltage of **100 kVp**.

respectively. We observed that the CC $[H_T]$ values of the breasts, stomach, thyroid, colon, and skin were higher when the female professional accompanied the 1-year-old patient at position 1. In this situation CC $[H_T]^{breast}$ was 1.90×10^{-2} (0.03 %) Sv/100 mAs (120 kVp) and 1.72×10^{-2} (0.03 %) Sv/100 mAs (100 kVp). The organs that received the highest CC $[H_T]$ values regardless of position and patient were the breasts.

In the same situation, a scenario was simulated with the professional using an apron lead, lead eyewear, and thyroid protector. In this case, the $CC[H_T]^{breast}$ was 4.79×10^{-4} (0.14 %) Sv/100 mAs (100 kVp) and 7.68×10^{-4} (0.14 %) Sv/100 mAs (120 kVp), as shown in Figs. 3 and 4, with approximately 96 % $CC[H_T]^{breast}$ reduction. As this is a radiosensitive organ with a large body mass, the use of the lead apron is extremely important. In addition to the breasts, other organs that also received higher doses were protected when the professional used the lead apron.

The thyroid gland is another organ that is radiosensitive. The highest $CC[H_T]^{thyroid}$ values were 1.25×10^{-2} (0.13 %) Sv/100 mAs for 120 kVp and 1.13×10^{-2} (0.13 %) Sv/100 mAs for 100 kVp, when the professional did not use PPE, in position 1 with the 1-year-old patient. With the use of a thyroid protector, the $CC[H_T]^{thyroid}$ values were reduced by approximately 93 %.

Figs. 5 and 6 show the CC $[H_T]$ values of the male professional, with and without PPE, and at tube voltages of 100 and 120 kVp, respectively. For male professionals, the organs with the highest CC $[H_T]$ values were the testicles, breasts, stomach, colon, and liver. The testicles in both positions and for all patients presented the highest $CC[H_T]^{testicles}$ values: 1.89×10^{-2} (0.09 %) Sv/100 mAs for 100 kVp and 2.05×10^{-2} (0.09 %) Sv/100 mAs for 120 kVp, when the professional accompanied the 1-year-old patient in position 1, being considered the most critical scenario. With the use of the lead apron, the $CC[H_T]^{testicles}$ values were 7.11×10^{-4} (0.15 %) Sv/100 mAs for 100 kVp and 1.05×10^{-3} (0.33 %) Sv/100 mAs for 120 kVp, presenting $CC[H_T]^{testicles}$ values reduced by approximately 96 %.

It is commonly noted that the organs shown in Figs. 3 and 6 are those that present the highest dose, among the most radiosensitive, have a high chance of presenting tissue reactions when exposed to ionizing radiation (Linet et al., 2010; Palm and Frida, 2017; ICRP, 2012). In addition, when professionals do not use PPE during patient follow-up, the highest $CC[H_T]$ values occur at position 1. In addition, as shown in Figs. 3 and 6, when (lead apron, lead eyewear, and thyroid shielding) is used, the CC $[H_T]$ values decreased by more than 90 %. Thus, it is recommended that professionals use PPE, and they must stay at position 2 (behind the gantry directed laterally).

To obtain the effective dose, the CC[E] values were multiplied by the air kerma measured experimentally by Costa et al. (2022). The E values in the professionals for all situations were calculated and are presented in Table 3.

It is observed that E values without PPE ranged from 5.26×10^{-2} mSv to 1.82×10^{-1} mSv, which can be explained due to variables between scenarios: size, BMI and gender of the patients, tube voltage and positions. The highest E values were for the professional in position 1, without PPE, with the 1-year-old patient and tube voltage of 120 kVp (Table 3).

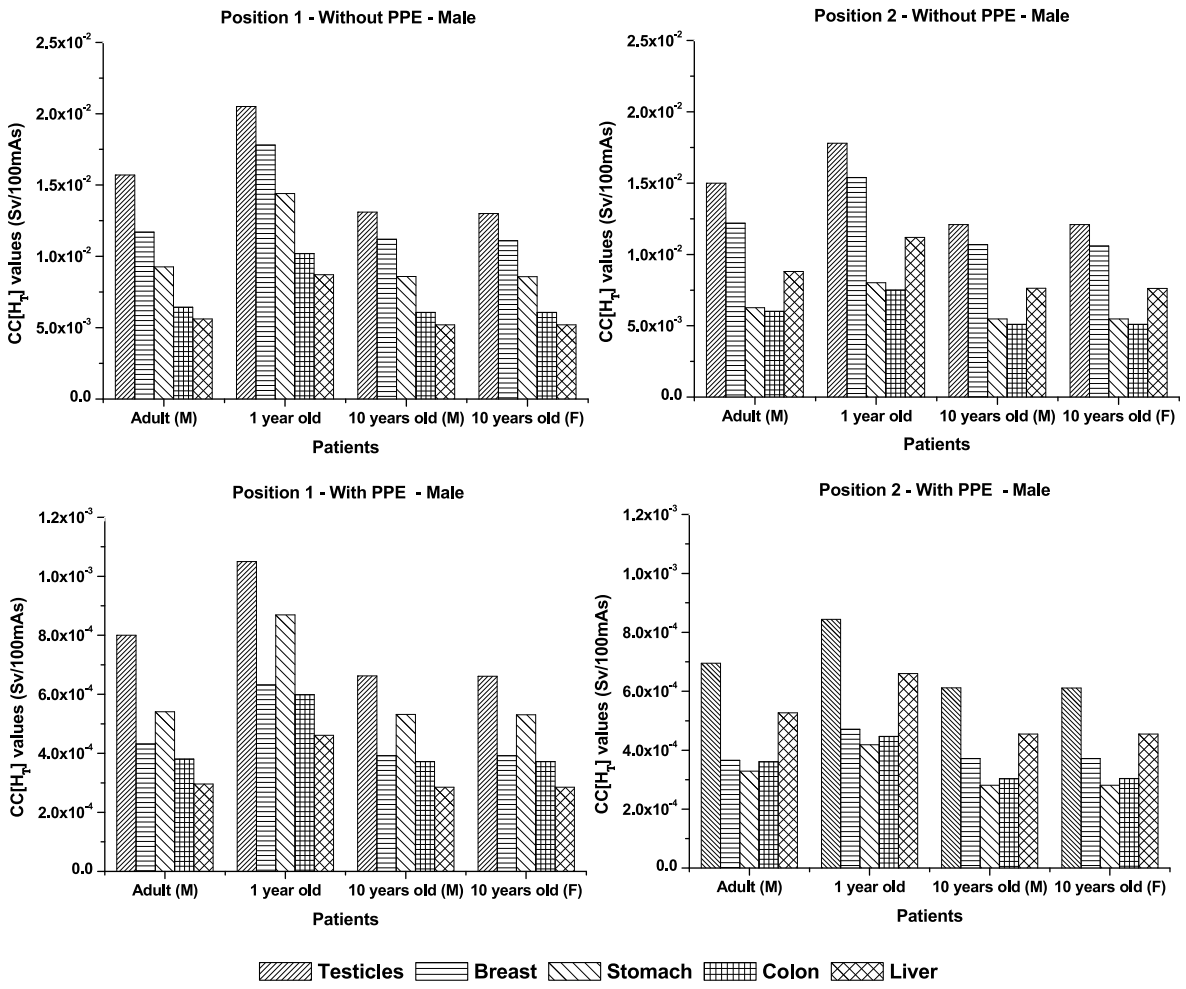

Fig. 6. Chart of the organs of the **male** professional who received the highest $CC[H_T]$ values, **without** e **with** PPE in positions 1 and 2 to follow the pediatric and adult patients, during the chest CT, considering a tube voltage of **120 kVp**.

Table 3
CC[E] values (mSv/Gy.100^{-1} mAs) and E (mSv) for the professional, with and without PPE, positioned in front of the gantry and facing the patient table (position 1), behind the gantry directed laterally (position 2), when monitoring and performing special care on pediatric (1- and 10-years old) and adult patients during diagnostic chest CT. The relative errors (%) are presented in parentheses.

Patient	Position 1				Position 2			
	Without PPE		With PPE		Without PPE		With PPE	
	CC[E]	E	CC[E]	E	CC[E]	E	CC[E]	E
100 kVp								
Adult	5.02 (0.03)	6.52×10^{-2} (0.03)	2.39×10^{-1} (0.12)	3.10×10^{-3} (0.12)	4.91 (0.03)	6.38×10^{-2} (0.03)	2.47×10^{-1} (0.12)	3.21×10^{-3} (0.12)
1 year old	7.54 (0.02)	9.80×10^{-2} (0.02)	3.68×10^{-1} (0.07)	4.78×10^{-3} (0.07)	6.05 (0.03)	7.86×10^{-2} (0.02)	3.20×10^{-1} (0.11)	4.16×10^{-3} (0.11)
10 years old (male)	4.45 (0.02)	5.78×10^{-2} (0.02)	2.27×10^{-1} (0.09)	2.95×10^{-3} (0.09)	4.05 (0.02)	5.26×10^{-2} (0.02)	2.17×10^{-1} (0.10)	2.82×10^{-3} (0.10)
10 years old (female)	4.53 (0.02)	5.89×10^{-2} (0.02)	2.29×10^{-1} (0.09)	2.97×10^{-3} (0.09)	4.13 (0.02)	5.37×10^{-2} (0.02)	2.18×10^{-1} (0.10)	2.84×10^{-3} (0.10)
120 kVp								
Adult	5.89 (0.03)	1.24×10^{-1} (0.03)	3.57×10^{-1} (0.09)	7.50×10^{-3} (0.09)	5.73 (0.03)	1.20×10^{-1} (0.03)	3.72×10^{-1} (0.10)	7.81×10^{-3} (0.10)
1 year old	8.68 (0.02)	1.82×10^{-1} (0.02)	5.52×10^{-1} (0.07)	1.16×10^{-3} (0.07)	6.95 (0.02)	1.46×10^{-1} (0.02)	4.62×10^{-1} (0.09)	9.71×10^{-3} (0.09)
10 years old (male)	5.27 (0.02)	1.11×10^{-1} (0.02)	3.36×10^{-1} (0.07)	7.05×10^{-3} (0.07)	4.77 (0.02)	1.00×10^{-1} (0.02)	3.22×10^{-1} (0.08)	6.75×10^{-3} (0.08)
10 years old (female)	5.27 (0.02)	1.11×10^{-1} (0.02)	3.36×10^{-1} (0.07)	7.05×10^{-3} (0.07)	4.76 (0.02)	1.00×10^{-1} (0.02)	3.21×10^{-1} (0.08)	6.75×10^{-3} (0.08)

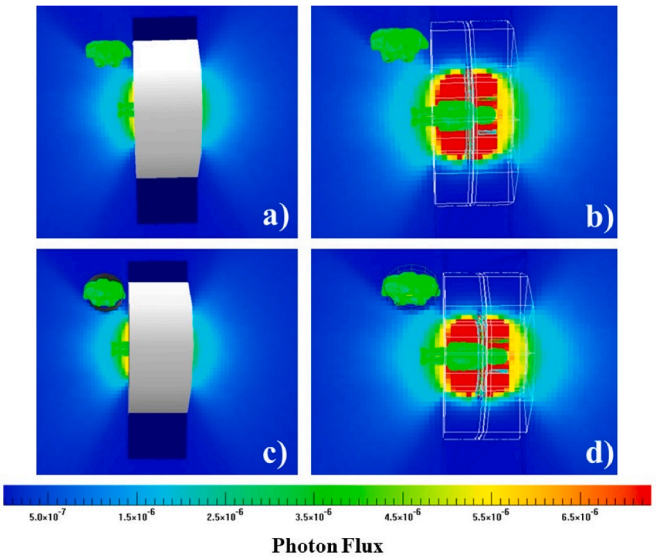

Fig. 7. Isodose map. The female professional, without PPE (a and b) and with PPE (c and d), positioned in front of the gantry and facing the table (position 1), during a 1-year-old patient follow-up in a chest CT.

In these scenarios, the effective doses were 9.80×10^{-2} mSv for 100 kVp, and 1.82×10^{-1} mSv for 120 kVp in position 1 and 7.86×10^{-2} mSv for 100 kVp and 1.46×10^{-1} mSv for 120 kVp, in position 2. Comparing the tube voltages of 100 kVp and 120 kVp, an increase of approximately 46 % was observed. Observing the two simulated positions, there was a 20 % dose reduction when the professional was in position 2. Furthermore, the use of PPE resulted in dose reductions of up to 91 % at both positions.

The scattered radiation in the CT room was evaluated for the critical scenario, in which the female professional accompanied the 1-year-old patient in position 1 and a tube voltage of 120 kVp. We evaluated the situations without PPE (Fig. 7a and b) and with PPE (Fig. 7c and d). The radiation levels were evaluated at a height of 130 cm from the floor with a 360° rotation of the X-ray tube.

Fig. 7 shows the dose levels of scattered radiation from the interaction of the incident X-ray beam with the patient's body and the CT equipment. Other organs and regions of the body absorb scattered radiation, resulting in undesirable doses for patients and professionals (Vázquez-Bañuelos et al., 2019; Campillo-Rivera et al., 2021; Dávila et al., 2018; Ron et al., 1995). We can see that in this position, as represented in Fig. 7, the dose received by the professional is quite high because areas around the CT equipment have a high level of scattered radiation (Palm and Frida, 2017; Ota et al., 2021).

Therefore, researchers have highlighted the importance of studying absorbed doses from scattered radiation (Heilmaier et al., 2016; Palm and Frida, 2017; Vázquez-Bañuelos et al., 2019; Campillo-Rivera et al., 2021; Dávila et al., 2018; Ron et al., 1995). Heilmaier et al., 2016, created a control and safety system called "traffic light," which determines different levels of radiation exposure at points in the CT room, which are established safety positions that the professional should stay in or risk positions that should be avoided (Heilmaier et al., 2016). Due to the high workload of the team, imposed by the high number of exams, and the uncomfortable clothing for biological risk, some professionals do not use or make inappropriate use of their PPE (Ota et al., 2021; Shafiee et al., 2020; Overhoff et al., 2020). Studies emphasize the efficiency of dose reduction when using radiological protection equipment, indicating the importance of using PPE (Heilmaier et al., 2016; Palm and Frida, 2017; Ota et al., 2021; Osanai et al., 2021; Dávila et al., 2018).

4. Conclusions

In this study, radiation doses were calculated for professionals of both genders during chest CT examinations, for patients with manual ventilation mechanism BVM. In this way, typical CT scenarios were simulated using Monte Carlo simulation and anthropomorphic phantoms, in which the different examination protocols, professional positioning, and the use of PPE were investigated.

The results obtained showed that the highest CC[E] values were for the professional positioned in front of the gantry and without the use of PPE, varying from 5.78×10^{-2} to 1.82×10^{-1} mSv, depending on the size of the patient and the tube voltage. The organs with the highest CC [H_T] values for the professional were the breast (females) and testicles (males).

We verified that the highest CC[H_T] and CC[E] values for the professionals occurred for positioning in front of the gantry and facing the patient table during a chest CT exam with a 1-year-old patient, without any PPE. In addition, it was concluded that the use of PPE reduced the CC[H_T] and E values by up to 91 %.

It is important to highlight that the estimation of the annual dose depends on different parameters, in which the ideal is to carry out more specific studies for each situation and protocol established by the institution. Because exposure to ionizing radiation poses risks to patients and professionals, it is necessary to emphasize the effects of radiological protection and compliance with safety standards for the medical staff.

CRediT authorship contribution statement

Monique F. Silva: Methodology, Software, Writing – original draft. **Ana L.O. Caixeta:** Software, Writing – original draft. **Samara P. Souza:** Software, Writing – original draft. **Otávio J. Tavares:** Software, Visualization. **Paulo R. Costa:** Methodology, Writing – review & editing. **William S. Santos:** Investigation, Validation. **Lucio P. Neves:** Data curation, Funding acquisition, Software, Writing – review & editing. **Ana P. Perini:** Conceptualization, Funding acquisition, Resources, Supervision, Writing – review & editing.

Declaration of competing interest

The authors declare that they have no known competing financial interests or personal relationships that could have appeared to influence the work reported in this paper.

Data availability

The data that has been used is confidential.

Acknowledgements

The authors would like to thank Dr. Richard Kramer for kindly providing the virtual anthropomorphic phantoms used in this work, and the Conselho Nacional de Desenvolvimento Científico e Tecnológico (CNPq) Brazilian agency for research projects 314520/2020-1 (L.P.N), 312124/2021-0 (A.P.P) and 309675/2021-9 (W.S.S); UNIVERSAL Project (407493/2021-2); MAI/DAI Project (403556/2020-1). The authors thank the Coordenação de Aperfeiçoamento de Pessoal de Nível Superior Brazilian Agency for Scholarships No. 88887.612310/2021-00 (M.F.S) and No. 88887.713182/2022-00 (A.L.O.C). This work was part of the Brazilian Institute of Science and Technology for Nuclear Instrumentation and Applications to Industry and Health (INCT/INAIS), CNPQ project 406303/2022-3. The authors would also like to thank the Fundação de Amparo à Pesquisa do Estado de Minas Gerais (FAPEMIG) for research projects APQ-02934-15, APQ-03049-15, APQ-04215-22, APQ-01254-23 and APQ-04348-23, and the Fundação de Amparo à Pesquisa do Estado de São Paulo (FAPESP) for research projects 2022/11457-0 and 2018/05982-0. S.P.S. received the FAPEMIG scholarship.

References

Abuelhia, E., Alghamdi, A., 2020. Evaluation of arising exposure of ionizing radiation from computed tomography and the associated health concerns. J. Radiat. Res. Appl. Sci. 13 (1), 295–300. https://doi.org/10.1080/16878507.2020.1728962.

Al-Hal, A.N., Lobriguito, A.M., Lagarde, C.S., 2003. Occupational doses during the injection of contrast media in pediatric CT procedures. Radiat. Protect. Dosim. 103, 169–172. https://doi.org/10.1093/oxfordjournals.rpd.a006129.

American College of Radiology. ACR–ASER–SCBT-MR–SPR Practice Parameter for the Performance of Pediatric Computed Tomography (CT). Available at: https://www.acr.org/-/media/ACR/Files/Practice-Parameters/CT-Ped.pdf. Accessed August 13, 2023.

Boone, J.M., 2010. Method for evaluating bow tie filter angle-dependent attenuation in CT: theory and simulation results. Med. Phys. 37 (1), 40–48. https://doi.org/10.1118/1.3264616.

Campillo-Rivera, G.E., Torres-Cortes, C.O., Vazquez-Bañuelos, J., Garcia-Reyna, M.G., Marquez-Mata, C.A., Vasquez-Arteaga, M., Vega-Carrillo, H.R., 2021. X-ray spectra and gamma factors from 70 to 120 kV X-ray tube voltages. Radiat. Phys. Chem. 184, 109437 https://doi.org/10.1016/j.radphyschem.2021.109437.

Cassola, V.F., De Melo Lima, V.J., Kramer, R., Khoury, H.J., 2009. FASH and MASH: female and male adult human phantoms based on polygon mesh surfaces: I. Development of the anatomy. Phys. Med. Biol. 55, 133–162. https://doi.org/10.1088/0031-9155/55/1/009.

Cassola, V.F., Kramer, R., De Melo Lima, V.J., Oliveira, C.A.B.L., Khoury, H.J., Vieira, J. W., Brown, K.R., 2013. Development of newborn and 1-year-old reference phantoms based on polygon mesh surfaces. J. Radiol. Prot. 33, 669–691. https://doi.org/10.1088/0952-4746/33/3/669.

Costa, P.R., Nersissian, D.Y., Salvador, F.C., Rio, P.B., Caldas, L.V.E., 2007. Gen- eration of calibrated tungsten target x-ray spectra: modified TBC model. Health Phys. 92 (1), 24–32. https://doi.org/10.1097/01.HP.0000231565.66004.f9.

Costa, P.R., Nersissian, D.Y., Umisedo, N.K., Gonzales, A.H.L., Fernández-Varea, J.M., 2022. A comprehensive Monte Carlo study of CT dose metrics proposed by the AAPM Reports 111 and 200. Med. Phys. 49 (1), 201–218. https://doi.org/10.1002/mp.15306.

Cristy, M., 1980. Mathematical phantoms representing children of various ages for use in estimates of internal dose. In: Report ORNL/NUREG/TM-367. Oak Ridge National Laboratory, Oak Ridge,Tenn., USA.

Dávila, H.O., Merchán, J.D., Carrillo, H.V., Ovalle, S.M., 2018. Assessment of the effectiveness of attenuation of Pb aprons by using TLD dosimetry and Monte Carlo calculations. Appl. Radiat. Isot. 138, 56–59. https://doi.org/10.1016/j.apradiso.2017.05.012.

De Melo Lima, V.J., Cassola, V.F., Kramer, R., De Oliveira, C.A.B.L., Khoury, H.J., Vieira, J.W., 2011. Development of 5 and 10-year-old pediatric phantoms based on polygon mesh surfaces. Med. Phys. 38, 4723–4736. https://doi.org/10.1118/1.3615623.

Ferrari, P., Jovanovic, Z., Bakhanova, E., Becker, F., Krstic, D., Jansen, J., Principi, S., Teles, P., Clairand, I., Knezevic, Ž., 2010. Absorbed dose in the operator's brain in interventional radiology practices: evaluation through KAP value conversion factors. Phys. Med. 76, 177–181. https://doi.org/10.1016/j.ejmp.2020.07.011.

Ferrari, P., Becker, F., Jovanovic, Z., Khan, S., Bakhanova, E., Principi, S., Krstic, D., Pierotti, L., Mariotti, F., Faj, D., Turk, T., Nikezic, D., Bertolini, M., 2019. Simulation of H p(10) and effective dose received by the medical staff in interventional radiology procedures. J. Radiol. Prot. 39 (3), 809–824. https://doi.org/10.1088/1361-6498/ab2c42.

Ferrari, P., Ginjaume, M., Hupe, O., O'Connor, U., Vanhavere, F., Bakhanova, E., Becker, F., Campani, L., Carinou, E., Clairand, I., Faj, D., Jansen, J., Jovanović, Z., Knežević, Ž., Krstić, D., Mariotti, F., Sans-Merce, M., Teles, P., Živković, M., 2022. Review: what is worth knowing in interventional practices about medical staff radiation exposure monitoring. Rev. Recent Outcomes EURADOS Working Group 12 Environments - MDPI 9 (4), 53. https://doi.org/10.3390/environments9040053.

Figueira, C., Becker, F., Blunck, C., DiMaria, S., Baptista, M., Esteves, B., Paulo, G., Santos, J., Tele, P., Vaz, P., 2013. Medical staff extremity dosimetry in CT fluoroscopy: an anthropomorphic hand voxel phantom study. Phys. Med. Biol. 58, 5433–5448. https://doi.org/10.1088/0031-9155/58/16/5433.

General Electric Company. Discovery CT750 HD. https://www.gehealthcare.com/-/jssmedia/documents/us-global/support/site-planning/computerized-tomography/pim/gehc-pim_discovery-ct-750hd-8x_5220253.zip?rev=a1f26071625c4f289e7217166ba1c52f&hash=4D51F3DE1D3796F47F17E109C6EA5226. Access in May 2023.

Gonzales, A.L., Tomal, A., Costa, P.R., 2015. Evaluation of characteristic-to-total spectrum ratio: comparison between experimental and a semi-empirical model. Appl. Radiat. Isot. 100, 27–31. https://doi.org/10.1016/j.apradiso.2015.01.011.

Gyekye, P.K., Becker, F., Mensah, S.Y., Emi-Reynolds, G., 2016. Optimisation of scatter radiation to staff during ct-fluoroscopy: Monte Carlo studies. Radiat. Protect. Dosim. 170, 393–397. https://doi.org/10.1093/rpd/ncw135.

Heilmaier, C., Mayor, A., Zuber, N., Fodor, P., Weishaupt, D., 2016. Improving radiation awareness and feeling of personal security of non-radiological medical staff by implementing a traffic light system in computed tomography. Röfo 188, 280–287. https://doi.org/10.1055/s-0041-110450.

Homayounieh, F., Holmberg, O., Umairi, R.A., Aly, S., Basevičius, A., Costa, P.R., Darweesh, A., Gershan, V., Ilves, P., Kostova-Lefterova, D., Renha, S.K., Mohseni, I., Rampado, O., Rotaru, N., Shirazu, I., Sinitsyn, V., Turk, T., Van Ngoc Ty, C., Kalra, M.K., Vassileva, J., 2021. Variations in CT utilization, protocols, and radiation doses in COVID-19 pneumonia: results from 28 countries in the IAEA study. Radiol. 298, E141–E151. https://doi.org/10.1148/radiol.2020203453.

ICRP, 2007. The 2007 recommendations of the international commission on radiological protection. Publication 103. Ann. ICRP 37 (2-4). https://www.icrp.org/docs/ICRP_Publication_103Annals_of_the_ICRP_37(2-4)-Free_extract.pdf.

ICRP, 2012. Statement on tissue reactions/early and late effects of radiation in normal tissues and organs – threshold doses for tissue reactions in a radiation protection context. Publication 118. Ann. ICRP 41 (1-2). https://journals.sagepub.com/doi/pdf/10.1177/ANIB_41_1-2.

Kobayashi, M., Koshida, K., Suzuki, S., Katada, K., 2012. Evaluation of patient dose and operator dose in swallowing CT studies performed with a 320-detector-row multislice CT scanner. Radiol. Phys. Technol. 5, 148–155. https://doi.org/10.1007/s12194-012-0148-3.

Kramer, R., Zankl, M., Williams, G., Drexler, G.O., 1982. Calculation of Dose from External Photon Exposure Using Reference Human Phantom and Monte Carlo Methods. Part I: the Male (ADAM) and Female (EVA) Adult Mathematical Phantoms. GSF-Bericht. S-885.

Kramer, R., Cassola, V.F., Khoury, H.J., Vieira, J.W., de Melo Lima, V.J., Brown, R.K., 2009. FASH and MASH: female and male adult human phantoms based on polygon mesh surfaces: II. Dosimetric calculations. Phys. Med. Biol. 55, 163–189. https://doi.org/10.1088/0031-9155/55/1/010.

Lee, C., Lodwick, D., Hurtado, J., Pafundi, D., Williams, L.J., Bolch, W.E., 2010. The UF family of reference hybrid phantoms for computational radiation dosimetry. Phys. Med. Biol. 55, 339–363. https://doi.org/10.1088/0031-9155/55/2/002.

Linet, M.S., Kim, K.P., Miller, D.L., Kleinerman, R.A., Simon, S.L., Berrington, G.A., 2010. Historical review of occupational exposures and cancer risks in medical radiation workers. Radiat. Res. 174, 793–808. https://doi.org/10.1667/RR2014.1.

McConn Jr., R.J., Gesh, C.J., Pagh, R.T., Rucker, R.A., Williams III, R.G., 2011. Compendium of material composition data for radiation Transport modeling. Pacific Northwest Nat. https://doi.org/10.2172/1023125. Laboratory. PNNL-15870 Rev. 1.

McKenney, S.E., Nosratieh, A., Gelskey, D., Yang, K., Huang, S.Y., Chen, L., Boone, J.M., 2011. Experimental validation of a method characterizing bow tie filters in CT scanners using a real-time dose probe. Med. Phys. 38 (3), 1406–1415. https://doi.org/10.1118/1.3551990.

McMillan, K., McNitt-Gray, M., Ruan, D., 2013. Development and validation of a measurement-based source model for kilovoltage cone-beam CT Monte Carlo dosimetry simulations. Med. Phys. 40 (11), 111907 https://doi.org/10.1118/1.4823795.

Mori, H., Koshida, K., Ishigamori, O., Matsubara, K., 2014. Investigation of qualitative and quantitative factors related to radiological exposure to nursing staff during computed tomography examinations. Health Phys. 107, S202–S210. https://doi.org/10.1097/HP.0000000000000186.

Nagamoto, K., Moritake, T., Nakagami, K., Morota, K., Matsuzaki, S., Nihei, S., Kamochi, M., Kunugita, N., 2021. Occupational radiation dose to the lens of the eye of medical staff who assist in diagnostic CT scans. Heliyon 7. https://doi.org/10.1016/j.heliyon.2021.e06063 e06063- e06074.

Ng, M.Y., Lee, E.Y.P., Yang, J., Yang, F., Li, X., Wang, H., Lui, M.M., Lo, C.S., Leung, B., Khong, P.L., Hui, C.K., Yuen, K.Y., Kuo, M.D., 2020. Imaging profile of the COVID-19 infection: radiologic findings and literature review. Radiol. Cardiothorac. Imag. 2 (1), e200034 https://doi.org/10.1148/ryct.2020200034.

Osanai, M., Sato, H., Sato, K., Kudo, K., Hosoda, M., Hosokawa, S., Kitajima, M., Tsushima, M., Fujita, A., Hosokawa, Y., 2021. Occupational radiation dose, especially for eye lens: $H_p(3)$, in medical staff members involved in computed tomography examinations. Appl. Sci. 11, 4448. https://doi.org/10.3390/app11104448.

Ota, J., Yokota, H., Kawasaki, T., Taoka, J., Kato, H., Chida, K., Masuda, Y., Uno, T., 2021. Evaluation of radiation protection methods for assistant staff during CT imaging in high-energy trauma: lens dosimetry with a phantom study. Health Phys. 120 (6), 635–640. https://doi.org/10.1097/HP.0000000000001391.

Overhoff, D., Weis, M., Riffel, P., Sudarski, S., Froelich, M.F., Fries, P., Schã¶Nberg, S., Gawlitza, J., 2020. Radiation dose of chaperones during common pediatric computed tomography examinations. Pediatr. Radiol. 50, 1078–1082. https://doi.org/10.1007/s00247-020-04681-6.

Palm, F., Frida, N., 2017. The importance of medical staff placement in CT examination rooms a study of the scattered radiation doses in CT examination rooms in. In: Da Nang (Vietnam): School of Health and Welfare. Jonkoping University. http://www.diva-portal.org/smash/get/diva2:1117348/FULLTEXT01.pdf. Access in Sept. 2021.

Radical Corporation, 2011. 10X6-3CT the Chamber for Computed Tomography Dose Index (CTDI), 4500054-3CT.

Ron, E., Lubin, J.H., Shore, R.E., Mabuchi, K., Modan, B., Pottern, L.M., Schneider, A.B., Tucker, M.A., Boice Jr., J.D., 1995. Thyroid cancer after exposure to external radiation: a pooled analysis of seven studies. Radiat. Res. 141, 259–277. https://doi.org/10.2307/3579003.

Shafiee, M., Rashidfar, R., Abdolmohammadi, J., Borzoueisileh, S., Salehi, Z., Dashtian, K., 2020. A study to assess the knowledge and practice of medical professionals on radiation protection in interventional radiology. Indian J. Radiol. Imag. 30, 64–69. https://www.ijri.org/text.asp?2020/30/1/64/281572.

Soares, M.R., Santos, W.S., Neves, L.P., Perini, A.P., Batista, W.O.G., Belinato, W., Maia, A.F., Caldas, L.V.E., 2019. Dose estimate for cone beam CT equipment protocols using Monte Carlo simulation in computational adult anthropomorphic phantoms. Radiat. Phys. Chem. 155, 252–259. https://doi.org/10.1016/j.radphyschem.2018.06.038.

Sookpeng, S., Martin, C.J., Kadman, B., 2019. Eye lens radiation doses to miscentering patients and health-care staff from head computed tomography. J. Radiol. Nurs. 38, 193–199. https://doi.org/10.1016/j.jradnu.2019.05.002.

Tamam, N., Salah, H., Almogren, K.S., Mahgoub, O., Saeed, M.K., Abdullah, Y., Tai, D.T., Omer, H., Sulieman, A., Bradley, D.A., 2023. Evaluation of patients' and occupational radiation risk dose during conventional and interventional radiology

procedures. Radiat. Phys. Chem. 207, 110818 https://doi.org/10.1016/j.radphyschem.2023.110818.

Terini, R.A., Nerssissian, D.Y., Campelo, M.C.S., Morice, V., Yoshimura, E.M., 2020. Compton spectrometry applied to clinical CT axial beams from tubes stopped and in revolution. Radiat. Phys. Chem. 171, 108734 https://doi.org/10.1016/j.radphyschem.2020.108734.

Turner, A.C., Zhang, D., Kim, H.J., DeMarco, J.J., Cagnon, C.H., Angel, E., Cody, D.D., Stevens, D.M., Primak, A.N., McCollough, C.H., McNitt-Gray, M.F., 2009. A method to generate equivalent energy spectra and filtration models based on measurement for multidetector CT Monte Carlo dosimetry simulations. Med. Phys. 36 (6), 2154–2164. https://doi.org/10.1118/1.3117683.

Vaño, E., Gonzalez, L., Beneytez, F., Moreno, F., 1998. Lens injuries induced by occupational exposure in non-optimized interventional radiology laboratories. Br. J. Radiol. 71, 728–733. https://doi.org/10.1259/bjr.71.847.9771383.

Vázquez-Bañuelos, J., Campillo-Rivera, G.E., García-Duran, Á., Rivera, E.R., Arteaga, M. V., Raigosa, A.B., Vega-Carrillo, H.R., 2019. Doses in eye lens, thyroid, and gonads, due to scattered radiation, during a CT radiodiagnosis study. Appl. Radiat. Isot. 147, 31–34. https://doi.org/10.1016/j.apradiso.2019.02.012.

Werner, C.J., Bull, J.S., Solomon, C.J., Brown, F.G., McKinney, G.W., Rising, M.E., Dixon, D.A., Martz, R.L., Hughes, H.G., Cox, L.J., Zukaitis, A.J., Armstrong, J.C., Forster, R.A., Casswel, L., 2018. MCNP6.2 Release Notes. Los Alamos National Laboratory report LA-UR-18-20808.

Yoriyaz, H., 2009. Método de Monte Carlo: princípios e aplicações em Física Médica Monte Carlo Method:principles and applications in Medical Physics. Rev. Bras. Fis. Med. 3, 141–149. https://doi.org/10.29384/rbfm.2009.v3.n1.p141-149.

Zamani, H., Kavousi, N., Masjedi, H., Omidi, R., Rahbar, S., Perota, G., Razavi, E., Zare, M.H., Abedi-Firouzjah, R., 2021. Estimation of diagnostic reference levels and achievable doses for pediatric patients in common computed tomography examinations: a multi-center study. Radiat. Protect. Dosim. 194 (4), 214–222. https://doi.org/10.1093/rpd/ncab093.